A DISSERTATION ON

Hydrogen Storage Capacity of Lithium terminated Carbon Chain

Submitted to
Department of Physics
Faculty of Science
Integral University, Lucknow, UP(INDIA)

In Partial Fulfillment

for the award of the
Degree of Master of Science

in Physics

By

Mohd Sharif

M.Sc. Physics(IV Semester)

Enroll No. 2100101715

UNDER THE SUPERVISION OF

Dr. HAROON

Assistant Professor
Department of Physics
Integral University
Lucknow, U.P.-226026(India)

INTEGRAL UNIVERSITY, DASAULI, KURSI ROAD, LUCKNOW

(2023)

Contents

List of Figures

List of Tables

Abstract

Predictions of the electronic and hydrogen storage properties of a linear chain of five carbon atoms terminated with two lithium atoms at both ends (Li_2C_5) have been made by using density functional theory. Owing to the alternation of the reactivity ofC_5 and Li_2C_5 with n, odd-even oscillations in their electronic properties are found. In contrast to C_5, the binding energies of H_2 molecules on Li_2C_5 are in (or close to) the ideal binding energy range (about $20\ to\ 40KJ/mol\ per\ H_2$).In addition, the H_2 gravimetric storage capacities of Li_2C_5 are the range of $10.7\ to\ 17.9wt\%$, satisfying the United States Department of energy(USDOE) ultimate target of $7.5\%wt\%$. The basis of our results, Li_2C_5 can be high-capacity hydrogen storage materials that can uptake and release hydrogen at temperatures well above the easily achieved temperature of liquid nitrogen.

Linear carbon chains (LCCs) have gained significant attention due to their unique electronic and hydrogen storage properties. The interaction of LCCs with various functional groups can significantly alter their behavior. In this study, we investigate the effect of lithium (Li) termination on the electronic and hydrogen storage properties of LCCs.

First, we employ first-principles calculations based on density functional theory (DFT) to examine the electronic structure of LCCs terminated with Li atoms. Our results show that Li termination induces a significant modification in the band structure of LCCs, leading to the formation of new energy states near the Fermi level. This alters the electrical conductivity and electronic transport properties of the system, making Li-terminated LCCs potential candidates for electronic device applications.

Furthermore, we explore the hydrogen storage capacity of Li-terminated LCCs. Hydrogen adsorption on carbon-based materials is an attractive strategy for energy storage. Our calculations reveal that Li termination enhances the physisorption of hydrogen molecules on LCCs by effectively polarizing and weakening the H-H bonds. This leads to improved hydrogen storage capacities compared to pristine LCCs. Moreover, the Li atoms act as anchoring sites, stabilizing the adsorbed hydrogen molecules.

We also investigate the hydrogen desorption process from Li-terminated LCCs. Our results indicate that the presence of Li atoms facilitates the release of stored hydrogen at lower temperatures, making Li-terminated LCCs potentially suitable for hydrogen release applications.

In summary, our study demonstrates that Li termination of LCCs has a profound impact on their electronic structure and hydrogen storage properties. The modified band structure enhances the electronic conductivity, while the presence of Li atoms improves the hydrogen storage capacity and facilitates hydrogen desorption. These findings offer valuable insights into the design and optimization of carbon-based materials for electronic and hydrogen storage applications

Introduction

As a pure energy carrier, hydrogen (H_2) possesses a variety of qualities. Due to its small weight, it has an energy density of $142\ MJ/kg$, which is roughly three times that of petrol. Additionally, water is extremely plentiful on Earth. More significantly, water vapor is released when hydrogen and oxygen are burnt. As the only waste product. Despite these benefits, there are still several issues that need to be resolved regarding the use of hydrogen. For instance, hydrogen is extremely combustible and will burst if it comes into touch with the atmosphere. Another issue is that it has extremely little energy per unit of volume ($0.0180MJ/L$), which is very little in comparison to petrol ($34.8MJ/L$). A lightweight storage medium is also needed because the storage of hydrogen for onboard uses has been popular over the past few years. These factors have made properly storing a significant amount of hydrogen in a compact, lightweight container the largest obstacle to the development of a hydrogen-based economy. [1-5]

The United States Department of Energy has followed the development of hydrogen storage materials for consumer automobiles over the years. For the gravimetric storage capabilities of onboard hydrogen storage materials for light-duty vehicles [5], the United States Department of Energy set the ultimate aim of $7.5wt\%$ in 2015. There are numerous ways to store hydrogen as of right now [1-4]. The conventional methods for storing hydrogen are the high-pressure method and the cryogenic method. In the high-pressure method, one adopts carbon fiber reinforced tanks, which can withstand very high pressures (e.g., $350\ to\ 700\ bar$), to store a large amount of completely recoverable hydrogen. In the cryogenic method, hydrogen is stored at very low temperatures (e.g.,$20K$), typically requiring an expensive liquid helium refrigeration system. Both of these methods are not suitable for onboard automobile applications, because of the associated risk, high cost, and heavy weight. Although the storage of hydrogen in metal hydrides appears to be a viable option, there are still issues to be solved, including this method's irreversibility, slow kinetics, and high desorption temperature. The storage of hydrogen via adsorption-based techniques in materials with high surface areas, such as carbon nanotubes, and metal-organic frameworks, is another promising graphene possibility. Because materials with a lot of surface area can absorb a lot of hydrogen, the resulting H_2 gravimetric storage capacities could be rather significant. However, these materials only function properly at very low temperatures because they attach H_2 molecules very weakly (i.e., mostly through van der Waal interactions).

In addition to other thermodynamic factors, the optimal binding energies of H_2 molecules on hydrogen storage materials should be in the range of roughly $20\ to\ 40kJ/mol$ per H_2 [6-8] for reversible hydrogen adsorption and desorption at ambient circumstances ($298K\ and\ 1\ bar$). The binding energies of H_2 molecules on high surface area materials are therefore being increased using a variety of innovative techniques to reach the aforementioned optimal range for ambient storage applications. The surface of the adsorbent is often altered through substitution doping, adatom adsorption, fictionalization, etc. The surface of the adsorbent is often altered through substitution doping, adatom adsorption, fictionalization, etc. to boost the H_2 adsorption binding energy.

Li adsorption stands out among them and is particularly appealing because of its light weight and ease of achieving a high gravimetric storage capacity. Also, take note of the fact that Li-adsorbed carbon materials have been demonstrated to have very high gravimetric storage capacities with improved H_2 adsorption binding energies and a charge-transfer driven polarization mechanism. [2,18]

Due to their distinctive electrical properties [10-24], linear carbon chains (C_5), which are composed of five carbon atoms bound with sp^1 hybridization (Figure 1), have recently received a lot of interest. Due to their one-dimensional ($1D$) structures and the practicality of synthesizing C_5 and their derivatives [24-30], it should be noted that$t\ C_5$ may be taken into consideration for hydrogen storage applications. Pt-terminated linear carbon chains have recently been created [28]. As previously indicated, Li-terminated linear carbon chains (Li_2C_5) can be suitable candidates for hydrogen storage materials because of a charge-transfer-driven polarization mechanism [2,18-20] (see Figure 5, Figure 7, Figure 9, Figure 11). (Li_2C_5) light elements (the C and Li atoms) made it possible to quickly acquire high gravimetric storage capacities. To our knowledge, however, no thorough study on the electronic and hydrogen storage properties of Li_2C_5 has been published. This may be because Li_2C_5 exhibits strong static correlation effects, which are frequently found in ($1D$) structures due to quantum confinement effects [25].

For systems with substantial static correlation effects, the popular Kohn-Sham density functional theory (KS-DFT) [26] with traditional semi-local [27], hybrid [28,29], and double-hybrid [30,40] density functionals may yield inaccurate findings. High-level ab initio multi-reference approaches are frequently required [33] for the precise prediction of these systems'

attributes. For big systems, however, accurate multi-reference calculations are unaffordable (particularly for geometry optimization).

We have recently developed thermally-assisted-occupation density functional theory (DFT) [34-36] for the study of large ground-state systems (e.g., containing up to a few thousand electrons) with strong static correlation effects to avoid the significant computational cost of high-level ab initio multi-reference methods. Unlike KS-DFT, DFT is a density functional theory with fractional orbital occupations, where strong static correlation is explicitly characterized by the entropy contribution, which is a function of the fake temperature and orbital occupancy numbers (see Eq. (26) of ref. 34). Take note that with DFT, the entropy contribution is absent. It is interesting to note that DFT is reduced to KS-DFT in the absence of severe static correlation effects and is as effective as KS-DFT for computations of single-point energy and analytical nuclear gradients. DFT, as opposed to KS-DFT, can therefore handle both single- and multi-reference systems in a more balanced manner. Additionally, DFT may use the XC density functional that is currently used in KS-DFT. DFT has been successfully applied to the study of several strongly correlated electron systems at the nanoscale [9,26-30] due to its computational effectiveness and reasonable accuracy for large systems with strong static correlation. These systems are typically regarded as "challenging systems" for traditional electronic structure methods (e.g., KS-DFT with conventional XC density functional and single- “ab initio” methods [32]). Accordingly, DFT can be an ideal theoretical method for studying the electronic properties of Li_2C_5. Besides, the orbital occupation numbers in DFT can be useful for examining the possible radical character of Li_2C_5. For the hydrogen storage properties, the interaction between H_2 and Li_2C_5 may involve dispersion (Vander waal) interactions, electrostatic interactions, and orbital interactions [3,7,26] the inclusion of dispersion corrections [26,38] in DFT is important for properly describing noncovalent interactions. Therefore, in this work, we adopt DFT with dispersion corrections [35] to study the electronic and hydrogen storage properties of Li_2C_5 with various chain lengths. In addition, the electronic properties of Li_2C_5 are also compared with those of C_5 to examine the role of Li termination.

Computational Detail

Gauss view:

In Gaussian09, Gauss View is a graphical tool for building molecules and reactive systems. It is utilized to create Gaussian09 input files and visually review the results.

Lithium terminated carbon chain

The pristine lithium terminated linear carbon chain is imported using software known as AVAGADRO in the XYZ coordinates for lithium terminated linear carbon chain. The molecular formula lithium terminated linear carbon chain is Li_2C_5 .

Basis Set: The "6-31+G(d')"

All calculations are performed with a development version of Gauusian09W using $b3lyp$/6-31+g(d'). Basis set with the fine grid EML [75,302]. The basis set "6-31+G(d')" is commonly used in quantum chemistry calculations and refers to the set of functions used to approximate the electronic wavefunctions of molecules. In the case of the B3LYP functional, it combines elements of Becke's three-parameter hybrid functional ($B3$) and the Lee-Yang-Parr correlation functional (LYP). Here are the computational details of the basis set B3LYP/6-31+G(d'). The basis set consists of two parts.

Atomic Orbitals (AO):

A). The basis set uses a combination of Gaussian-type orbitals (GTOs) to describe the atomic orbitals. It includes a set of contracted GTOs for each atom, where each contracted GTO is composed of a linear combination of primitive GTOs. The "6-31" part represents the level of contraction used for the atomic orbitals.

b). Polarization Functions: The "+G(d')" part represents the inclusion of polarization functions, which are additional basis functions added to improve the description of electronic correlation effects. In the case of 6-31+G(d'), "d'" indicates the inclusion of diffuse functions in addition to standard polarization functions. The diffuse functions help capture the electronic behavior in diffuse regions of molecules.

1. Geometry Optimization: The B3LYP/6-31+G(d') method can be used for geometry optimization, where the positions of atoms are adjusted to find the lowest energy configuration of the molecule.
2. Energy Calculations: The B3LYP/6-31+G(d') method can also be used for energy calculations, which involve determining the total electronic energy of a molecule. This can be done for ground state energies or excited states, depending on the specific calculation.
3. Post-Processing: After performing calculations using the B3LYP/6-31+G(d') method, further analysis can be conducted to study various molecular properties, such as molecular orbitals, bond lengths, vibrational frequencies, and more.

   It's worth noting that computational details may vary depending on the specific software or computational chemistry package used. Different basis sets and functionals may also be employed based on the nature of the system being studied and the level of accuracy desired.

B3LYP:

All calculations were performed using the Gaussian09 quantum chemistry software [31]. A Gaussian basis set was employed throughout the calculations. In computational chemistry, the hybrid density functional theory (DFT) approach known as $B3LYP$ is frequently employed. It combines the Lee-Yang-Parr correlation functional (LYP) and Becke's three-parameter exchange functional ($B3$). For a variety of chemical systems, the $B3LYP$ technique strikes a fair balance between precision and computational expense The $B3LYP$ method is a popular hybrid density functional within the framework of density functional theory (DFT). It combines the Becke three-parameter exchange functional ($B3$) with the Lee-Yang-Parr correlation functional (LYP). The $B3LYP$ method is widely used in computational chemistry to calculate the electronic structure and properties of molecules. The $B3LYP$ functional includes both the exchange and correlation contributions to the total energy of the system. The exchange term accounts for the quantum mechanical effect of electron exchange, where electrons avoid each other due to their indistinguishability. The correlation term captures the electron-electron interactions beyond the exchange effects, accounting for the repulsion or attraction between electrons. The $B3LYP$ functional is considered a hybrid functional because

it incorporates a fraction of the Hartree-Fock exchange (exact exchange) into the density functional. This mixing of Hartree-Fock exchange with the exchange-correlation function enhances the description of both short-range and long-range electron-electron interactions.

The $B3LYP$ functional has been shown to provide reasonably accurate results for a wide range of molecular systems, including organic molecules, transition metal complexes, and biological systems. It often yields good predictions for molecular geometries, vibrational frequencies, reaction energies, and electronic spectra. However, it is important to note that the performance of the $B3LYP$ functional can vary depending on the specific system and property being studied. While the $B3LYP$ method has been widely used and remains popular, it is worth mentioning that there are other functionals available in DFT with different strengths and weaknesses. Researchers often select the appropriate function based on the system under investigation and the level of accuracy required for the specific application

Calculation with Gaussian:

Geometry Optimization:

Using $B3LYP$, begin by optimizing the molecule geometry. Finding the atomic configuration that corresponds to the system's minimal energy is necessary for this. Atom locations are modified iteratively to optimize geometry until the forces acting on each atom are minimal.

Density Functional Theory:

Density field theory is the most common technique used for computing structures of atoms, molecules, crystals, and their interactions “ab initio”. This is a density-based technique theory, not a wave function-based theory. The main aim is to obtain an approximate solution of the Schrödinger equation to determine the ground state of a many-state problem. Within this theory, the property of many-electron systems is determined by using fundamentals. In this case, density DFT accounts for the electric correlation function.

DFT was first put on a firm theoretical footing by Walter Kohn and Pierre Hohenberg in the framework of two Hohenberg Kohn theorem (It states that the ground energy of many electrons system can be calculated by the functional of electron density which is the function of time and space. The Hohenberg kohn theorem asserts that the density of any system determines all ground state properties of the system. If the electron density functional of the

system is known, total energy can be estimated. Density Functional Theory (DFT) is a computational method used to study the electronic structure and properties of atoms, molecules, and solids. It is based on quantum mechanics and provides a powerful tool for understanding and predicting various properties of materials, such as energies, structures, charge densities, and electronic spectra. In DFT, the central quantity of interest is the electron density, which represents the probability distribution of electrons in a system. The theory aims to find the electron density that minimizes the total energy of the system. This is achieved by solving the Kohn-Sham equations, which are a set of self-consistent equations derived from a fictitious system of non-interacting electrons.

The basic principles of DFT are rooted in the Hohenberg-Kohn theorems. These theorems state that the ground-state electron density uniquely determines the ground-state energy and vice versa. This establishes the foundation for DFT to describe many-body quantum systems in terms of electron density rather than solving the complicated many-electron wavefunction. One of the key components in DFT is the exchange-correlation functional, which accounts for the electron-electron interactions beyond the non-interacting system. The exchange term represents the quantum mechanical effect of electron exchange, while the correlation term accounts for the repulsion or attraction between electrons due to their interactions. Various approximations and functionals exist to approximate the exchange-correlation term, and their accuracy depends on the specific system and property being studied. DFT has become a widely used method in theoretical and computational chemistry, condensed matter physics, materials science, and related fields. It allows researchers to investigate a wide range of systems, from small molecules to complex materials and surfaces. Despite its approximations, DFT has been successful in providing accurate predictions and understanding of many physical and chemical phenomena, making it an indispensable tool for modern research and development.

Model System

Figure 1 Linear carbon atom chain with Li terminated atoms at the ends (C_5Li_2), Pink ball represents Li atom, Grey ball represents a carbon atom

The model system (as shown in Figure 1) contains a linear carbon chain having five atoms terminated with two lithium atoms at both ends. Among carbon materials, linear carbon chains (C_n), consisting of *n* carbon atoms bonded with sp1 hybridization have recently attracted much attention owing to their unique electronic properties [10,24]. Note that C_n may be considered for hydrogen storage applications due to their one-dimensional (1D) structures and the feasibility of synthesis of C*n* and their derivatives [13, 19]. Recently, Pt-terminated linear carbon chains have been synthesized [17]. As mentioned above, due to a charge-transfer-induced polarization mechanism [2, 52-54], Li-terminated linear carbon chains (Li_2C_n) can be good candidates for hydrogen storage materials (see Figure 5 to Figure 12). Because of the light elements (i.e., C and Li atoms) in Li_2C_n, high gravimetric storage capacities could be easily achieved. However, to the best of our knowledge, there has been no comprehensive study on the electronic and hydrogen storage properties of Li_2C_n in the literature, possibly due to the presence of strong static correlation effects in Li_2C_n (commonly occurring in 1D structures due to quantum confinement effects)[25].

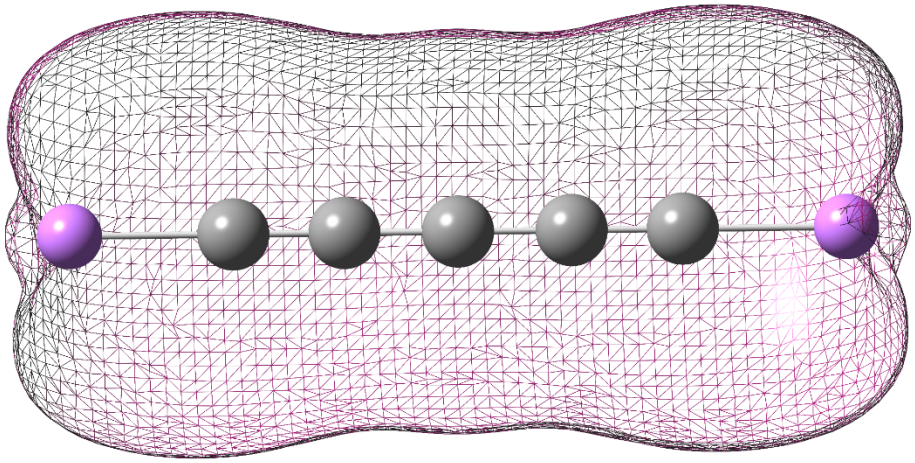

Figure 2 Total charge density isosurfaces of Li terminated carbon chain.

The optimized structure of the model system shown in Figure 1 is presented with the isosurfaces plot in Figure 2 showing the total charge density. Total charge density isosurfaces are graphical representations of the electron density distribution in a molecule or solid. They provide a visual depiction of the regions in space where the electron density is concentrated. The visualization of total charge density isosurfaces is a valuable tool in understanding molecular and solid-state systems, aiding in the interpretation of chemical bonding, reactivity, and various other properties.

Results and Discussion

Hydrogen storage properties

As pure carbon materials bind H_2 molecules very weakly (i.e., mainly governed by van der Waal interactions), they are unlikely to be promising hydrogen storage materials at ambient conditions [6], Similarly, C_5 are not ideal for ambient storage applications, since the binding energies of H_2 molecules remain small. In addition, the number of H_2 molecules that can be adsorbed on C_5 is quite limited, due to the repulsive interaction between the adsorbed H_2 molecules at short distances [62]. Consequently, the more the adsorbed H_2 molecules, the less the average H_2 binding energy on C_5. Therefore, C_5 cannot be high-capacity hydrogen storage materials at ambient conditions.

Here, we investigate the hydrogen storage properties of Li_2C_5. As illustrated in(Figure 5, Figure 7, Figure 9, Figure 11), at the ground-state geometry of Li_2C_5, xH_2 molecules ($x = 0, 2, 4, 6, 8$) are initially placed on various possible sites around each Li atom, and the structures are subsequently optimized to obtain the most stable geometry. All the H_2 molecules are found to be adsorbed molecularly to the Li atoms. The average H_2 binding energy, $E_b(H_2)$, on Li_2C_5 evaluated by

$$E_b(H_2) = \frac{E_{Li_2C_5} + 2xE_{H_2} - E_{Li_2C_5-2xH_2}}{2x}$$

where E_{H_2} is the total energy of H_2, and $E_{Li_2C_5-2xH_2}$ is the total energy of Li_2C_5 with xH_2 molecules adsorbed on each Li-atom. Subsequently, $E_b(H_2)$ is corrected for BSSE using standard counterpoise correction. As shown in figure12 $E_b(H_2)$ is in the range of $19\ to\ 27\ kJ/mol\ per\ H_2$ for $x = 1-4$, in the range of $18\ to\ 19\ kJ/mol$ per H_2 for $x = 5$, and about $16\ kJ/mol\ per\ H_2$ for $x = 6$, falling in (or close to) the ideal binding energy range.

To assess if the binding energies of successive H_2 molecules are also in (or close to) the ideal binding energy range (i.e., not just the average H_2 binding energy), the binding energy of the y^{th} H_2 molecule ($y = 1-5$), $E_{b,y}(H_2)$, on Li_2C_5, is evaluated by

$$E_{b,y}(H_2) = (E_{Li_2C_5-2(y-1)H_2} + 2E_{H_2} - E_{Li_2C_5-2yH_2})/2$$

Similarly, $E_{b,y}(H_2)$ is also corrected for BSSE using a standard counterpoise correction60 .As shown in Fig. 7(b), $E_{b,y}(H_2)$ is in the range of $16\ to\ 27\ kJ/mol\ per\ H_2$ for ($y = 1–4$), in the range of $11\ to\ 12\ kJ/mol\ per\ H_2$ for $y = 5$, and less than $5\ kJ/mol\ per\ H_2$ for $y = 6$. Therefore, while the first four H_2 molecules can be adsorbed on Li_2C_5 in (or close to) the ideal binding energy range, the fifth and sixth H_2 molecules are only weakly adsorbed (i.e., appropriate only for storage at very low temperatures). To assess the types of non-covalent interactions between H_2 and Li_2C_5, we compute the atomic charge on each Li atom for Li_2C_5 with xH_2 molecules ($x = 0, 2, 4, 6, 8$) adsorbed on each Li-atom (see **Figure** 3), using the in which atomic charges are fitted to reproduce the molecular electrostatic several points around the molecule.

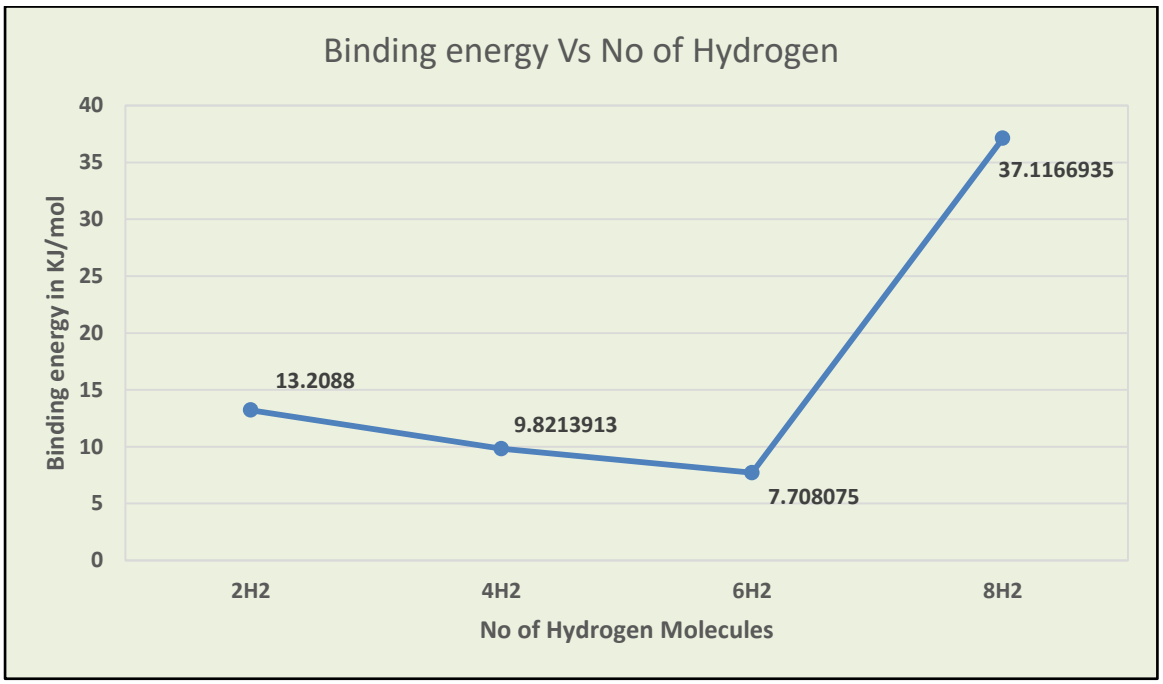

Figure 3 Binding energy Vs number of H_2

Binding energy in KJ/mol	Number of H_2 molecules
13.2088	$2H_2$
9.8213913	$4H_2$
7.708075	$6H_2$
37.1166935	$8H_2$

Figure 4 Average binding energy per molecule

Adsorption of Two H_2 Molecules

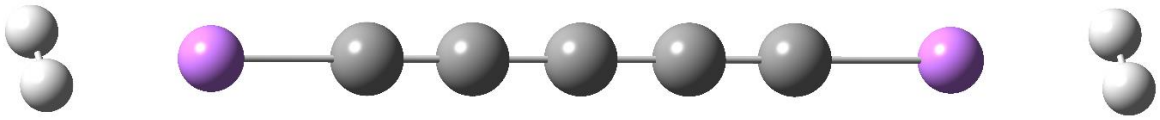

Figure 5 Li_2C_5 with two H_2 molecules adsorbed on each Li atom. (Purple ball represents the Li atom, the grey ball represents the carbon atom, and the white ball represents the hydrogen atom)

In this figure3 Li_2C_5 adsorbed two molecules of hydrogen on each Li atom. The optimized structure is shown in Figure 5.

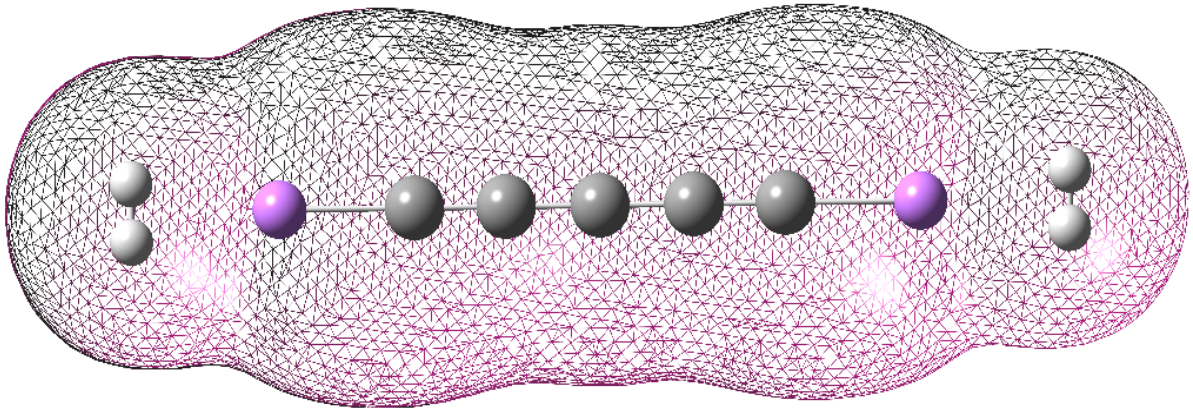

Figure 6 Charge density isosurfaces of two H_2 molecules adsorbed around Li atoms at the end of the carbon chain.

Adsorption of four H_2 molecules

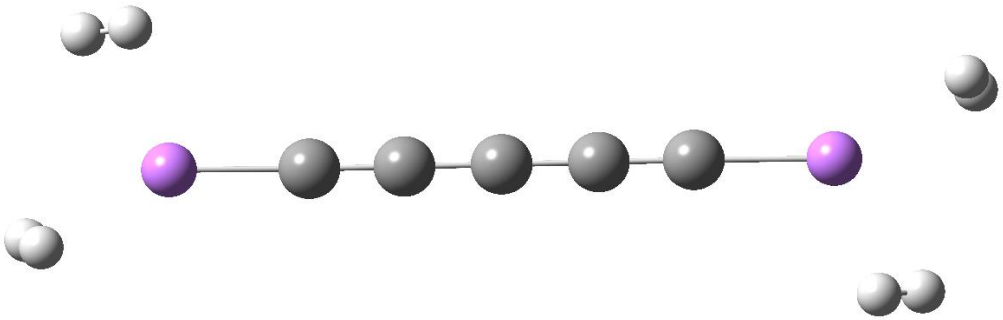

Figure 7 Li_2C_5 with four H_2 adsorbed on each Li atom (The purple ball represents the Li atom, the grey ball represents the carbon atom, and the white ball represents the hydrogen atom).

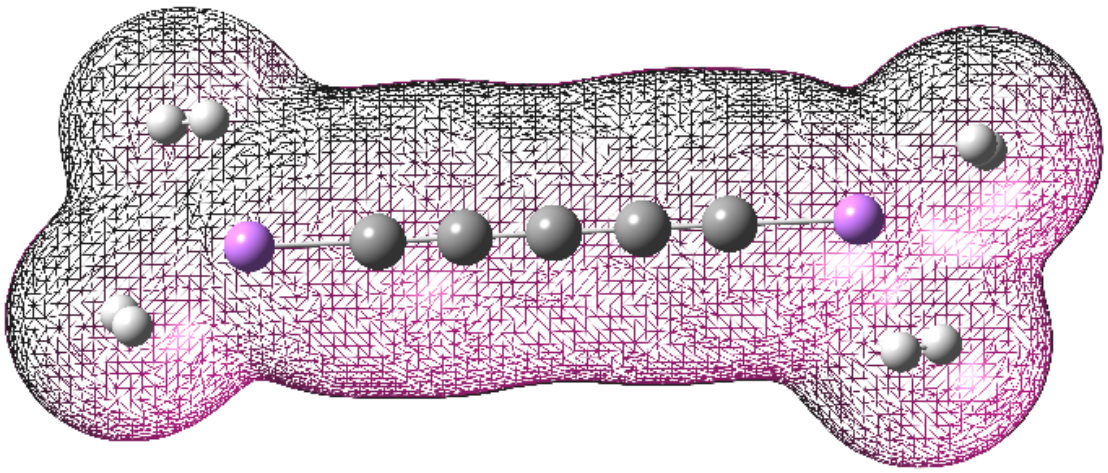

Figure 8 Charge density isosurfaces of Li terminated carbon chain.

Adsorption of Six H_2 Molecules

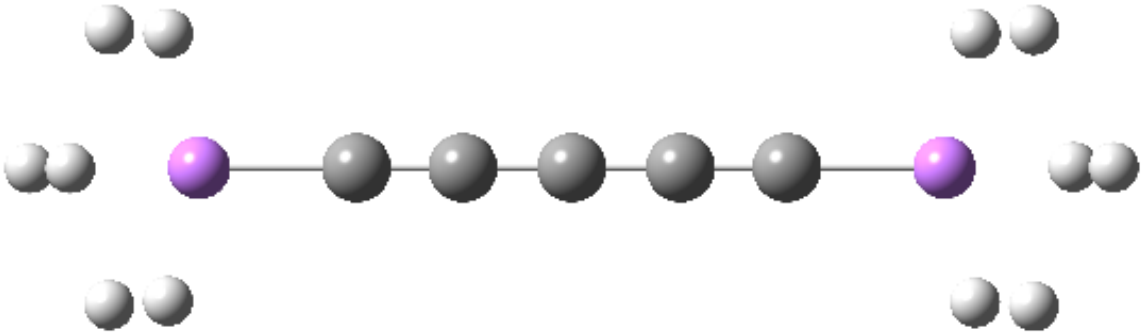

Figure 9 Li_2C_5 with six H_2 molecules adsorbed on each Li atom (The purple ball represents the Li atom, the grey ball represents the carbon atom, and the white ball represents the hydrogen atom).

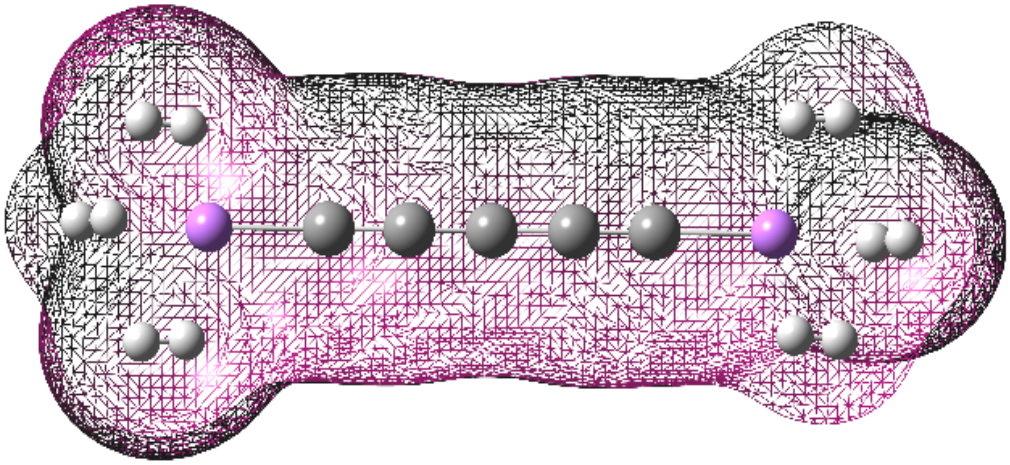

Figure 10 charge density isosurfaces of six H_2 adsorbed at the end of Li terminated carbon chain.

Adsorption of Eight H_2 Molecules

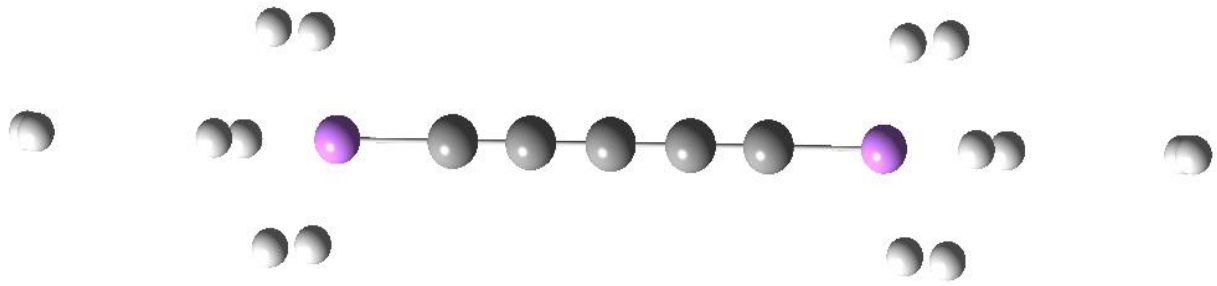

Figure 11 Li_2C_5 with six H_2 at the ends of the Li terminated carbon chain. The purple ball represents the Li atom, the grey ball represents the carbon atom, the white ball represents the hydrogen atom.

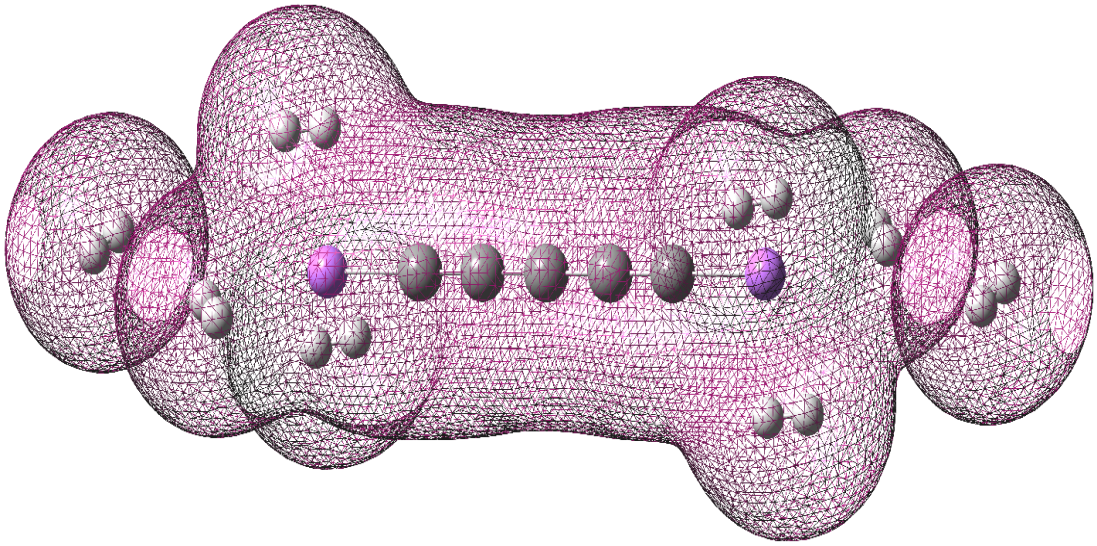

Figure 12 charge density isosurfaces of eight H_2 adsorbed at the ends of Li terminated carbon chain.

We plot the charge density isosurfaces of C_5 and Li_2C_5 with xH$_2$ molecules ($x = 0,2,4,6,8$) adsorbed on each Li atom see **Figure** 5 to **Figure** 12. As an electronegativity of C is much higher than that of Li, the transfer of electronic charge in Li_2C_5 to C_5 resulting in a positive charge of $(0.83524 - 0.58157)e$ on each Li atom in Li_2C_5. The positively charged Li atom can interact with more than one H_2 molecule, the positive charge on Li decreases for the subsequent adsorption of H_2 molecules. This type of adsorption can be attributed to the polarization of H_2 molecules by the positively charged Li atom (i.e., charge -induced dipole interaction) [2,18-20], leading to the enhanced H_2 energy and high hydrogen uptake in Li_2C_5. When the number of adsorbed H_2 molecules is large, there is a significant overlap of the Li and H_2 charge densities, enhancing orbital interaction [3,7,37]. This suggests that orbital interactions should also be responsible for the H_2 binding energy, especially when a large

number of H_2 molecules are adsorbed on the Li atom. Interestingly, there is no overlap (or slight overlap) between the charge density of the two additional H_2 molecules after $6H_2$ are being absorbed this can be observed in Figure 11 and **Figure** 12. The charge densities of these H_2 molecules, after the sixth H_2 molecules are only weakly adsorbed. Accordingly, the non-covalent interactions between H_2 molecules and Li_2C_5 should involve charge induced dipole interactions, orbitals interactions and vander-Waal interactions.

The natural charge on the Li atoms obtained from the Summary of Natural Population Analysis (NBO charge), as the number H_2 molecules are adsorbed on the carbon chain. The values of the charges are shown in **Table 1** below, the variation of natural charge is also plotted in **Figure** 13.

Table 1 Variation of Charge on Li atoms (obtained from Natural Population Analysis) due to adsorption of H2 molecules.

No of H_2 molecules	Natural Charge on Li atom (e)
0	0.83524
2	0.73324
4	0.63228
6	0.58231
8	0.58157

As clear from Figure 13 the natural charge on Li atoms gradually decreases due to the enhanced orbital interactions, when the H2 molecules are adsorbed on the Li atom, a small fraction of electronic charge is transferred between the Li atom and the adsorbed H2 molecules.

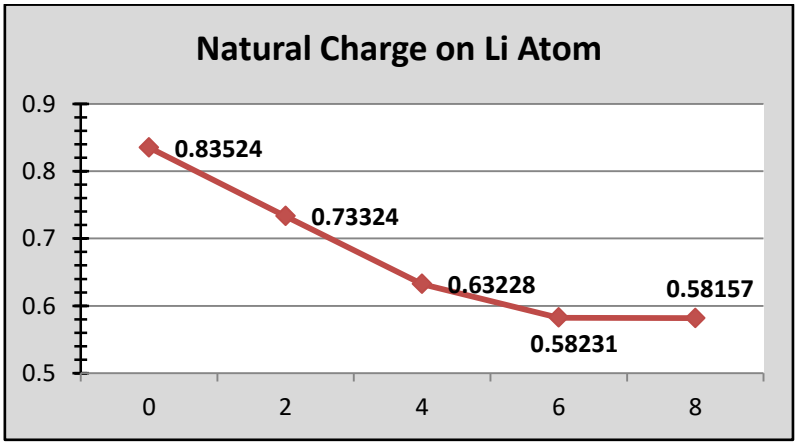

Figure 13 Natural charge on each Li atom (shown on the y-axis) for Li_2C_5 with xH2 (x=2, 4, 6, 8) molecules adsorbed on each Li atom (shown on the x-axis).

Gravimetric Storage Capacity

As Li_2C_5 can bind up to $8H_2$ molecules (i.e., each Li atom can bind up to $4H_2$ molecules) with the average and successive H_2 binding energies in (or close to) the ideal binding energy range, the corresponding H_2 gravimetric storage capacity, Cg, is calculated using the expression below

$$C_g = \frac{8M_{H_2}}{M_{Li_2C_5} + 8M_{H_2}}$$

Here, $M_{Li_2C_5}$ is the mass of Li_2C_5 and M_{H_2} is the mass of H_2. Note that C_g is $17.9\ wt\%$ for n, $15.8\ wt\%$ satisfying the United States Department of Energy's ultimate target of $7.5\ wt\%$. Based on the observed trends for Li_2C_5, the maximum number of H_2. molecules that can be adsorbed on each Li atom with the average and successive H_2, binding energies in (or close to) the ideal binding energy range should be, regardless of the chain length. Therefore, the C_g value of Li_2C_5 should decrease as the chain length increases. Note, however, that the C_g values obtained here may not be directly compared to the United States Department of Energy target value, which refers to the complete storage system (i.e., with the storage material, enclosing tank, insulation, piping, etc.), Nevertheless, since the C_g values obtained here are much higher (especially for the shorter Li_2C_5) than the United States Department of Energy's ultimate target, the complete storage systems based on Li_2C_5 are likely to be high-capacity hydrogen storage materials that can uptake and release hydrogen at temperatures well above the temperature of liquid nitrogen.

Electronic properties

Binding Energy:

Spin-unrestricted $B3YLP$ calculations are carried out for the lowest singlet and triplet energies of C_5/ Li_2C_5 on the corresponding geometries that were fully optimized at the same theoretical level to get the ground state of C_5/Li_2C_5. The energy difference between the lowest triplet (T) and singlet (S) states of C_5/ Li_2C_5 is used to compute the singlet-triplet energy gap (ST) of C_5/ Li_2C_5. The ground states of C_5 and Li_2C_5 are singlets for all of the chain lengths examined.

The lowest spin-restricted state of C_5/Li_2C_5 should have the same spin-restricted and spin-unrestricted energies for the precise theory [34-36, 41] due to the symmetry restriction. We also do spin-restricted calculations for the lowest singlet energies on the corresponding optimized geometries to evaluate the potential symmetry-breaking consequences. Within the numerical precision of our calculations, the spin-restricted and spin-unrestricted B3LYP energies for the lowest singlet state of C_5/Li_2C_5 are found to be nearly identical, suggesting that virtually no asymmetry-breaking effects occur in our spin-unrestricted $B3LYP$ calculations. To assess the energetic stability of terminating Li atoms, the Li binding energy, $E_b\,(Li)$, on C_5 is computed using

$$E_b(Li) = \frac{E_{C_5} + 2E_{Li} - E_{Li_2C_5}}{2},$$

where is the total energy of C_5 , E_{Li} is the total energy of Li, and $E_{Li_2C_5}$is the total energy of Li_2C_5, $E_b(Li)$ is subsequently corrected for the basis set superposition error (BSSE) using the counterpoise correction[39] where C_5 is considered as one fragment, and the $2Li$ atoms are considered as the other fragment, C_5 can strongly bind the Li atoms with the binding energy range of $258\ to\ 357\ kJ/mol\ per\ Li$. At the ground state (i.e., the lowest singlet state) geometry of C_5/ Li_2C_5 (with N electrons), the vertical ionization potential ($IP_v = E_{N-1} - E_N$), vertical electron affinity($EA_v = E_N - E_{N+1}$), and fundamental gap ($E_g = IP_v - EA_v = E_{N+1} + E_{N-1} - 2E_N$) are obtained with multiple energy-difference calculations, with E_N being the total energy of the N-electron system.

von Neumann entropy:

In our case, for the spin-restricted situation, we can find the symmetrized von Neumann entropy (this helps in examining the possible radical character of C_5/Li_2C_5) of a ground-state molecule that can be expressed as

$$S_{vN} = -\sum_{i=1}^{\infty}\left\{\frac{f_i}{2}\ ln\left(\frac{f_i}{2}\right) + \left(1-\frac{f_i}{2}\right)\ ln\left(1-\frac{f_i}{2}\right)\right\}$$

where f_i (i.e., a number between 0 and 2) is the occupation number of the i-th orbital of the Ground-State molecule, obtained with spin-restricted DFT calculations. Note that f_i is closely related to the corresponding natural orbital occupation number, which can also be obtained at finite temperature using a Thermal Assisted Occupation DFT (TAO-DFT) [42-45]. For a ground-state molecule possessing a nonradical nature, the occupation numbers associated with all orbitals are very close to either 0 or 2, yielding vanishingly small values of von Neumann entropy. Nonetheless, for a Ground-State molecule with a significant radical nature, the active orbital occupation numbers can deviate significantly from 0 and 2 (for example, 0.2–1.8); hence, the corresponding von Neumann entropy S_{vN} values can greatly increase as the number of active orbitals increases and/or the active orbital occupation numbers are closer to 1 [44-51]. For a system without a strong static correlation f_i are close to either 0 or 1, S_{vN} provides insignificant contributions, while for a system with strong static correlation (f_i are fractional for active orbitals, and are close to either 0 or 1 for others).

As shown in Figure 14, the S_{vN} values of the molecule Li_2C_5 increases for the adsorption of H_2 molecules up to six, due to an increase in the number of active orbitals. For eight hydrogen molecules the value of S_{vN} is less than that of six hydrogen molecules, though the value of S_{vN} is expected to increase due to the participation of active orbitals in addition to active orbitals. The decrease in the value of S_{vN} for the eight hydrogen molecules can be understood from the charge density distribution. As shown in Figure 10 the charge density surface of the Li_2C_5 along with six hydrogen molecule shows a closed and connected surface depicting a bound system with hydrogen molecules adsorbed around the lithium atoms. While in case eight hydrogen molecules as shown in Figure 12 the charge density surface seems disconnected for two hydrogen molecules present at the left and right extreme of the lithium atoms. The two hydrogen molecules at extreme positions are at a large distance as compared to the six hydrogen molecules which form a closely bound system around the lithium atoms within a suitable distance favorable for the adsorption.

Within the present approach for the calculation the hydrogen adsorption can be governed easily, but the Kohn Sham-DFT with conventional exchange (XC) density functional can be unreliable for the properties of systems with strong static correlation effects, and accurate multi-reference calculations are prohibitively expensive for large systems (e.g., the longer C_5 and Li_2C_5). In addition, due to the alteration of the reactivity of C_n and Li_2C_n with n, it is highly desirable to adopt an electronic structure method that can provide a balanced performance for both single and multi-reference systems, this can be well justified by the use of TAO-DFT.

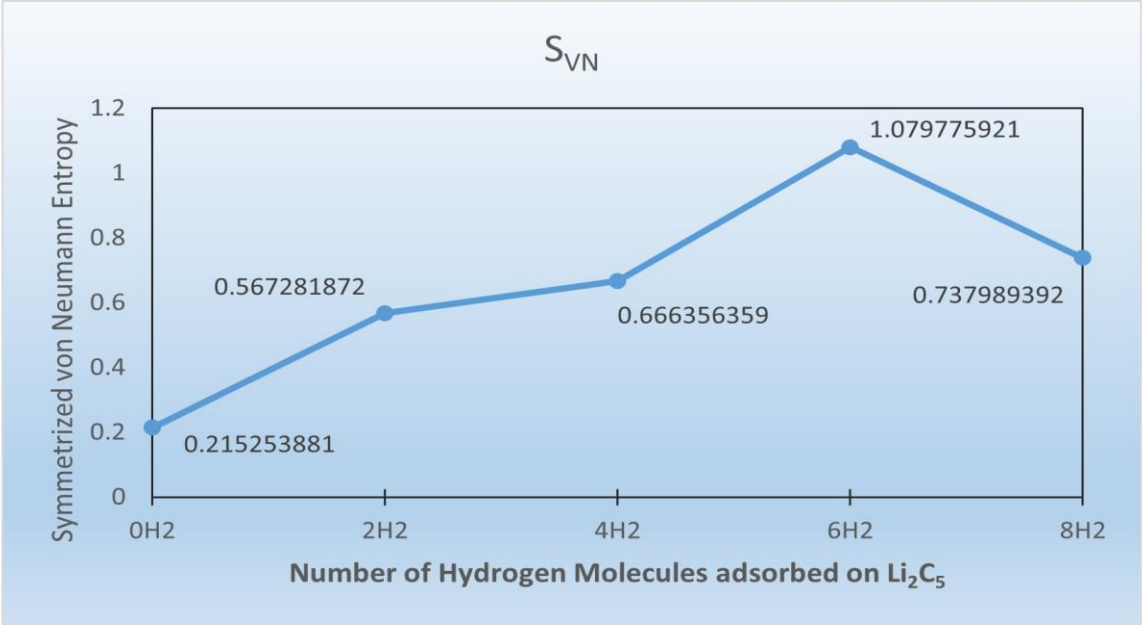

Figure 14 Symmetrized von Neumann vs no of H_2 molecules adsorbed on Li_2C_5

As shown in Table **2** to **Table** 6, the population of active orbitals for the Li_2C_5 molecules and the same molecules upon adsorption of hydrogen molecules in with an increase in numbers of two. The number of active orbitals for Li_2C_5 are 127 and increase as 138, 147, 152 and 157 respectively for the addition of hydrogen molecules. As can be seen from **Table 2** there are 13 vacant orbitals (occupancy zero) for the molecule Li_2C_5. Upon hydrogen adsorption the redistribution of population takes place in all active orbitals due to correlations and the number of vacant orbitals decreases. The number of vacant orbitals upon hydrogen adsorption is either absent or few (due to some symmetry adopted by the molecules upon adsorption). In all cases, the occupancies vary between 0-2 and it is hard to find any orbitals with occupancy exactly 1 or 2. All the orbitals have fractional values of occupancy due to correlations in the molecule.

In **Figure** 15, the natural population of orbitals for $Li_2C_5$with and without hydrogen adsorption is plotted for data shown in **Table 2** to **Table 6**. Some peaks with maximum heights represent nearly double occupancies while some peaks with heights shorter than 1 show partial/fractional occupancies.

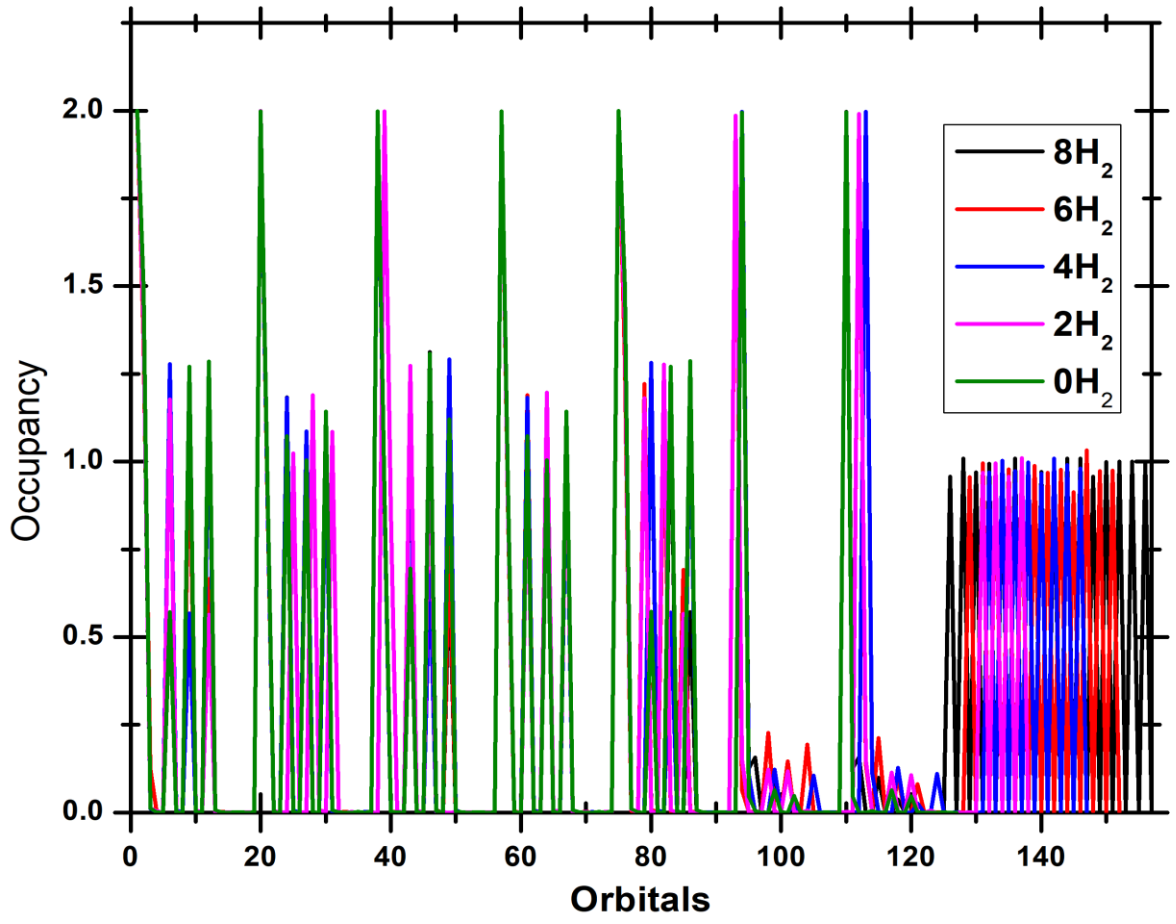

Figure 15 NATURAL POPULATIONS: Natural atomic orbital occupancies of Li_2C_5 with and without H_2 adsorption.

Table 2 NATURAL POPULATIONS of the Orbitals for Li_2C_5 molecule.

Occupancy of the Orbitals for Li_2C_5 (No H_2 Molecule Adsorbed)					
S. NO	**Occupancy**	**S. NO**	**Occupancy**	**S. NO**	**Occupancy**
1	**1.99943**	**46**	**1.30696**	**91**	**0.00066**
2	**1.49502**	**47**	**0.00507**	**92**	**0.00002**
3	**0.01146**	**48**	**0.00015**	**93**	**0.00047**
4	**0.00086**	**49**	**1.12013**	**94**	**1.99524**
5	**0.00003**	**50**	**0.00283**	**95**	**0.04462**
6	**0.57185**	**51**	**0.00077**	**96**	**0.00468**
7	**0.00049**	**52**	**0**	**97**	**0.00001**
8	**0.00005**	**53**	**0.00095**	**98**	**0**

9	**1.27029**	**54**	**0.00074**	**99**	**0.06328**
10	**0.00193**	**55**	**0.00001**	**100**	**0.0009**
11	**0.0002**	**56**	**0.00039**	**101**	**0.00001**
12	**1.2857**	**57**	**1.99888**	**102**	**0.04723**
13	**0.00654**	**58**	**0.93785**	**103**	**0.00143**
14	**0.00059**	**59**	**0.00141**	**104**	**0.00003**
15	**0**	**60**	**0.00015**	**105**	**0**
16	**0.00063**	**61**	**1.07261**	**106**	**0.00006**
17	**0.00066**	**62**	**0.00077**	**107**	**0.00036**
18	**0.00002**	**63**	**0.00015**	**108**	**0**
19	**0.00048**	**64**	**1.00334**	**109**	**0**
20	**1.99888**	**65**	**0.00059**	**110**	**1.99527**
21	**0.93784**	**66**	**0.00022**	**111**	**0.04621**
22	**0.00145**	**67**	**1.14273**	**112**	**0.00016**
23	**0.00016**	**68**	**0.00704**	**113**	**0.00006**
24	**1.07261**	**69**	**0.00153**	**114**	**0.00467**
25	**0.00076**	**70**	**0**	**115**	**0.00002**
26	**0.00016**	**71**	**0.00016**	**116**	**0**
27	**1.00334**	**72**	**0.00176**	**117**	**0.06349**
28	**0.0006**	**73**	**0.00001**	**118**	**0.00069**
29	**0.00021**	**74**	**0.00288**	**119**	**0.00001**
30	**1.14274**	**75**	**1.99943**	**120**	**0.04682**
31	**0.007**	**76**	**1.49495**	**121**	**0.00125**
32	**0.00149**	**77**	**0.0113**	**122**	**0.00004**
33	**0**	**78**	**0.00104**	**123**	**0**
34	**0.00016**	**79**	**0.00003**	**124**	**0.00006**
35	**0.00176**	**80**	**0.57188**	**125**	**0.00036**
36	**0.00001**	**81**	**0.00048**	**126**	**0**
37	**0.0029**	**82**	**0.00002**	**127**	**0.00007**
38	**1.99877**	**83**	**1.27044**		
39	**0.90861**	**84**	**0.00194**		
40	**0.0022**	**85**	**0.00004**		
41	**0.00133**	**86**	**1.28649**		
42	**0.00003**	**87**	**0.00669**		
43	**0.69556**	**88**	**0.00031**		
44	**0.00058**	**89**	**0**		
45	**0**	**90**	**0.00063**		

Table 3 NATURAL POPULATIONS of the Orbitals for Li_2C_5 molecule ($2H_2$ Molecule Adsorbed).

Occupancy of the Orbitals for Li_2C_5 ($2H_2$ Molecule Adsorbed)							
S.No	**Occupancy**	**S.No**	**Occupancy**	**S.No**	**Occupancy**	**S.No**	**Occupancy**
1	1.99927	46	1.12065	91	0.00091	136	0.00192
2	1.39582	47	0.00338	92	0.00021	137	1.01026
3	0.01296	48	0.00142	93	1.98647	138	0.00112
4	0.00466	49	0	94	0.15287		
5	0.00006	50	0.00110	95	0.00146		
6	1.17719	51	0	96	0.00013		
7	0.00194	52	0.00073	97	0.00002		
8	0.00081	53	0	98	0.12250		
9	1.26883	54	0.00093	99	0.00108		
10	0.00732	55	0.00124	100	0.00001		
11	0.00088	56	0.0003	101	0.11766		
12	0.56385	57	1.9987	102	0.00144		
13	0.00120	58	0.90525	103	0.00004		
14	0.00004	59	0.00234	104	0.00533		
15	0.00101	60	0.00013	105	0.00005		
16	0	61	1.02289	106	0		
17	0.00089	62	0.00070	107	0.00027		
18	0.00074	63	0.00047	108	0		
19	0.00019	64	1.19644	109	0.00001		
20	1.9991	65	0.00601	110	0.00156		
21	0.93187	66	0.00371	111	0.00037		
22	0.00342	67	1.08518	112	1.99081		
23	0.00276	68	0.00103	113	0.14923		
24	0.0001	69	0.00019	114	0.00211		
25	1.0241	70	0.00178	115	0.00010		
26	0.00067	71	0	116	0.00003		
27	0.00041	72	0.00017	117	0.11439		
28	1.1893	73	0.00203	118	0.00103		
29	0.00657	74	0.00049	119	0.00001		
30	0.00185	75	1.99916	120	0.10621		
31	1.08556	76	1.38851	121	0.00122		
32	0.00088	77	0.00785	122	0.00006		

33	0.00019	78	0.00025	123	0.00525		
34	0.00177	79	1.18039	124	0.00005		
35	0	80	0.00207	125	0		
36	0.00017	81	0.00080	126	0.00027		
37	0.00050	82	1.27636	127	0.00000		
38	0.00009	83	0.00734	128	0.00001		
39	1.99832	84	0.00076	129	0.00090		
40	0.86019	85	0.56611	130	0.00023		
41	0.00284	86	0.00084	131	0.96774		
42	0.00039	87	0.00006	132	0.00229		
43	1.27306	88	0.00100	133	0.99554		
44	0.00615	89	0	134	0.00129		
45	0.00048	90	0.00090	135	0.95729		

Table 4 NATURAL POPULATIONS of the Orbitals for Li_2C_5 molecule ($4H_2$ Molecule Adsorbed)

Occupancy of the Orbitals for Li_2C_5 ($4H_2$ Molecule Adsorbed)							
S. No	Occupancy	S. No	Occupancy	S. No	Occupancy	S. No	Occupancy
1	1.99932	46	0.68514	91	0	136	0.97356
2	1.3995	47	0.00059	92	0.00061	137	0.00044
3	0.01026	48	0.00001	93	0.00027	138	0.99792
4	0.0011	49	1.29186	94	1.9967	139	0.00053
5	0.00007	50	0.00762	95	0.10854	140	0.96589
6	1.27852	51	0.0002	96	0.00124	141	0.0003
7	0.0066	52	0.00092	97	0.00004	142	1.00849
8	0.00142	53	0.00074	98	0.00004	143	0.0005
9	0.56793	54	0	99	0.12208	144	0.99093
10	0.00098	55	0.00032	100	0.00113	145	0.00043
11	0.00018	56	0.00018	101	0.00013	146	0.98114
12	1.18534	57	1.99864	102	0.02366	147	0.0004
13	0.00173	58	0.90477	103	0.00022		
14	0.00054	59	0.00172	104	0.00002		
15	0.00089	60	0.00028	105	0.10563		
16	0.00102	61	1.18198	106	0.00065		
17	0	62	0.0054	107	0.00003		
18	0.00061	63	0.00094	108	0.00047		
19	0.00027	64	1.08644	109	0.00022		

20	1.99864	65	0.00072	110	0.00008		
21	0.90535	66	0.0002	111	0.00043		
22	0.00169	67	1.02622	112	0.00041		
23	0.00029	68	0.00064	113	1.99674		
24	1.18201	69	0.00016	114	0.11333		
25	0.00542	70	0.00017	115	0.0013		
26	0.00097	71	0.00184	116	0.00004		
27	1.08645	72	0	117	0.00004		
28	0.00074	73	0.00173	118	0.1273		
29	0.0002	74	0.00079	119	0.00131		
30	1.02631	75	1.99932	120	0.00014		
31	0.00065	76	1.40264	121	0.02619		
32	0.00018	77	0.01073	122	0.0002		
33	0.00018	78	0.00105	123	0.00002		
34	0.00184	79	0.00006	124	0.10991		
35	0	80	1.28121	125	0.00073		
36	0.00173	81	0.00661	126	0.00003		
37	0.00079	82	0.00142	127	0.00076		
38	1.99876	83	0.57021	128	0.00029		
39	0.88642	84	0.00086	129	0.0001		
40	0.00261	85	0.00028	130	0.0001		
41	0.00069	86	1.18683	131	0.00035		
42	0.00005	87	0.00169	132	0.96913		
43	1.13738	88	0.00048	133	0.00041		
44	0.00323	89	0.0009	134	1.00249		
45	0.00098	90	0.00102	135	0.00055		

Table 5 NATURAL POPULATIONS of the Orbitals for Li_2C_5 molecule ($6H_2$ Molecule Adsorbed).

Occupancy of the Orbitals for Li_2C_5 ($6H_2$ Molecule Adsorbed)							
S.No	Occupancy	S.No	Occupancy	S.No	Occupancy	S.No	Occupancy
1	1.99922	46	1.21572	91	0.00124	136	0.00007
2	1.34042	47	0.00523	92	0.00031	137	0.96848
3	0.1246	48	0.00016	93	1.97403	138	0.00081
4	0.00147	49	0.7754	94	0.06419	139	0.98773
5	0.00007	50	0.00139	95	0.00234	140	0.0007

6	**1.25171**	**51**	**0.0002**	**96**	**0.00157**	**141**	**0.96802**
7	**0.00742**	**52**	**0.00073**	**97**	**0.00003**	**142**	**0.00006**
8	**0.00121**	**53**	**0.0009**	**98**	**0.2272**	**143**	**0.97717**
9	**1.10615**	**54**	**0.00001**	**99**	**0.00108**	**144**	**0.00055**
10	**0.00212**	**55**	**0.00041**	**100**	**0.00005**	**145**	**0.91248**
11	**0.00055**	**56**	**0.00009**	**101**	**0.14554**	**146**	**0.00094**
12	**0.66615**	**57**	**1.99856**	**102**	**0.00033**	**147**	**1.03276**
13	**0.00085**	**58**	**0.88685**	**103**	**0.00002**	**148**	**0.00182**
14	**0.00206**	**59**	**0.0026**	**104**	**0.19353**	**149**	**0.97334**
15	**0.00099**	**60**	**0.00037**	**105**	**0.00132**	**150**	**0.00021**
16	**0.00091**	**61**	**1.18935**	**106**	**0.00005**	**151**	**0.97408**
17	**0.00001**	**62**	**0.00539**	**107**	**0.00103**	**152**	**0.00088**
18	**0.0005**	**63**	**0.00237**	**108**	**0.00048**		
19	**0.00012**	**64**	**1.01638**	**109**	**0.00084**		
20	**1.99859**	**65**	**0.00065**	**110**	**0.00074**		
21	**0.8984**	**66**	**0.00067**	**111**	**0.00091**		
22	**0.00189**	**67**	**1.07243**	**112**	**1.98487**		
23	**0.00021**	**68**	**0.00104**	**113**	**0.13595**		
24	**1.1792**	**69**	**0.00107**	**114**	**0.00125**		
25	**0.00482**	**70**	**0.00164**	**115**	**0.21195**		
26	**0.00119**	**71**	**0.00044**	**116**	**0.00077**		
27	**1.02846**	**72**	**0.00001**	**117**	**0.00005**		
28	**0.00064**	**73**	**0.0021**	**118**	**0.10088**		
29	**0.00023**	**74**	**0.00056**	**119**	**0.00028**		
30	**1.07451**	**75**	**1.99871**	**120**	**0.00004**		
31	**0.00065**	**76**	**1.27835**	**121**	**0.08098**		
32	**0.00084**	**77**	**0.00429**	**122**	**0.00083**		
33	**0.00163**	**78**	**0.00085**	**123**	**0.00006**		
34	**0.00043**	**79**	**1.22132**	**124**	**0.00091**		
35	**0.00001**	**80**	**0.0055**	**125**	**0.00101**		
36	**0.00211**	**81**	**0.00403**	**126**	**0.00018**		
37	**0.00056**	**82**	**1.14778**	**127**	**0.00072**		
38	**1.99879**	**83**	**0.00343**	**128**	**0.00079**		
39	**0.8821**	**84**	**0.00144**	**129**	**0.95538**		
40	**0.00285**	**85**	**0.69181**	**130**	**0.00027**		
41	**0.00098**	**86**	**0.0025**	**131**	**0.99497**		

42	0.00022	87	0.00237	132	0.00029		
43	1.13302	88	0.00088	133	0.97238		
44	0.00392	89	0.00108	134	0.00043		
45	0.00089	90	0.00003	135	0.9784		

Table 6 NATURAL POPULATIONS of the Orbitals for Li_2C_5 molecule ($8H_2$ Molecule Adsorbed).

Occupancy of the Orbitals for Li_2C_5 ($8H_2$ Molecule Adsorbed)							
S.No	Occupancy	S.No	Occupancy	S.No	Occupancy	S.No	Occupancy
1	1.99928	46	1.31255	91	0.00001	136	1.0089
2	1.38056	47	0.00765	92	0.00077	137	0.0007
3	0.0102	48	0.00013	93	0.0002	138	0.99388
4	0.00124	49	0.68098	94	1.99653	139	0.00026
5	0.00005	50	0.00055	95	0.12512	140	0.97014
6	1.27005	51	0	96	0.1575	141	0.00022
7	0.00601	52	0.00072	97	0.00077	142	0.95743
8	0.00129	53	0.00092	98	0.00025	143	0.00024
9	1.20808	54	0	99	0.09883	144	1.00921
10	0.00217	55	0.00042	100	0.00017	145	0.00071
11	0.00073	56	0.00007	101	0.00002	146	1.00898
12	0.57118	57	1.99862	102	0.03748	147	0.00071
13	0.00066	58	0.9038	103	0.00005	148	0.95741
14	0.00036	59	0.00159	104	0.00001	149	0.00024
15	0.00103	60	0.00032	105	0.00057	150	0.99869
16	0.00088	61	1.18321	106	0.00034	151	0.00002
17	0.00001	62	0.00521	107	0.00047	152	1.00064
18	0.00077	63	0.00093	108	0.00012	153	0
19	0.0002	64	1.02442	109	0.00024	154	0.99976
20	1.99862	65	0.00065	110	1.99654	155	0
21	0.9038	66	0.00021	111	0.12548	156	0.99955
22	0.00159	67	1.08516	112	0.15778	157	0.00001
23	0.00032	68	0.00072	113	0.00079		
24	1.18317	69	0.00018	114	0.00025		
25	0.00522	70	0.00189	115	0.09866		
26	0.00093	71	0.00017	116	0.00014		
27	1.02446	72	0	117	0.00001		
28	0.00065	73	0.00207	118	0.03729		

29	**0.00021**	**74**	**0.00049**	**119**	**0.00005**		
30	**1.08514**	**75**	**1.99928**	**120**	**0.00001**		
31	**0.00072**	**76**	**1.38088**	**121**	**0.00058**		
32	**0.00018**	**77**	**0.01022**	**122**	**0.00034**		
33	**0.00189**	**78**	**0.00123**	**123**	**0.00047**		
34	**0.00017**	**79**	**0.00005**	**124**	**0.00012**		
35	**0**	**80**	**1.27009**	**125**	**0.00024**		
36	**0.00207**	**81**	**0.006**	**126**	**0.9573**		
37	**0.00049**	**82**	**0.00129**	**127**	**0.00025**		
38	**1.99877**	**83**	**1.20818**	**128**	**1.00927**		
39	**0.88508**	**84**	**0.00216**	**129**	**0.00072**		
40	**0.00268**	**85**	**0.00072**	**130**	**0.96949**		
41	**0.00073**	**86**	**0.57104**	**131**	**0.00022**		
42	**0.00006**	**87**	**0.00066**	**132**	**0.99437**		
43	**1.13955**	**88**	**0.00037**	**133**	**0.00026**		
44	**0.00354**	**89**	**0.00103**	**134**	**0.95757**		
45	**0.00095**	**90**	**0.00088**	**135**	**0.00024**		

Conclusion

As a result of recent developments in DFT, there are advanced versions of DFT methods such as the TAO-DFT, the present approach within KS-DFT has been utilized to examine the hydrogen storage over a simple molecule Li_2C_5. The optimum hydrogen storage has been explored to the exchange-correlation within B3LYP. We have obtained the electronic properties of Li_2C_5, including the binding energies, Mulliken Charges, charge density surfaces, and natural population analysis. We have also obtained gravimetric storage capacity and symmetrized von Neumann entropy. Hydrogen storage properties upon successive H_2 storage has been determined. The Li_2C_5 has been found to have radical nature. The present approach may have some significant limitations which can be further analyzed with a higher version of DFT methods, but the present approach for our model system can however predict several important features (with computationally effectiveness) and give an insight to investigate the model further.

According to our findings, Li_2C_5 can bind $6H_2$ molecules ($3H_2$ molecules on Li atom) clearly, and the addition of further two hydrogen molecules making upto the adsorption of eight molecules may be possible. The average and subsequent H_2 binding energies being in the optimal range of roughly $20 - 40\ kJ/mol\ per\ \ H_2$ molecule. As a result, Li_2C_5 H_2 gravimetric storage capacities fall between 13.9 and $17.7 wt\%$, satisfying the United States Department of Energy's ultimate aim of 7.5 $wt\%$. As a result, consequently, Li_2C_5 can be used as high-capacity hydrogen storage materials.

Future research may take into account conducting a thorough analysis of these devices' electronic and hydrogen storage characteristics. Since the successful synthesis of linear carbon chains [26, 27] and Pt-terminated linear carbon chains [28] the realization of hydrogen storage materials based on Li_2C_5 should be possible and is now available to experimenters.

References

[1]1. Schlapbach, L.Zuttel, A Hydrogen-storage materials for mobile applications, *nature 414,353-358 (2001).*

[2] Jena, P. Materials for the hydrogen storage: past. Present and future. *J.Phys.chem.Lett.206-211 (2011).*

[3] Park, N.et al.Progress on first-principles-based materials design for *hydrogen storage. PNAS109,19893-19899 (2012)*

[4] Dalebrook,A.F.,Gan,W.,Grasemann,M., Moret, S.&Laurenczy,G. Hydrogen storage: beyond conventional methods. *Che. common. 49, 8735-8751 (2013).*

[5] U. S. Department of Energy, Target explanation document: onboard hydrogen storage for light-duty fuel cell vehicles. Technical report. Available at: https://energy.gov/eere/fuelcells/hydrogen-storage (Accessed: January 2017) (2015).

[6] Bhatia, S. K. & Myers, A. L. Optimum conditions for adsorptive storage. *Langmuir 22, 1688–1700 (2006).*

[7]. Lochan, R. C. & Head-Gordon, M. Computational studies of molecular hydrogen binding affinities: the role of dispersion forces, electrostatics, and orbital interactions. *Phys. Chem. Chem. Phys. 8, 1357–1370 (2006).*

[8]. Sumida, K. et al. Impact of metal and anion substitutions on the hydrogen storage properties of M-BTT metal-organic frameworks. *J. Am. Chem. Soc. 135, 1083–1091 (2013).*

[9]. Seenithurai, S. & Chai, J.-D. Effect of Li adsorption on the electronic and hydrogen storage properties of acenes: a dispersion corrected TAO-DFT study. *Sci. Rep. 6, 33081 (2016).*

[10]. Fan, Q. & Pfeiffer, G. V. Theoretical study of linear Cn (n=6–10) and HCnH (n=2–10) molecules. *Chem. Phys. Lett. 162, 472–478 (1989).*

[11]. Heimann, R. B. In Carbyne and Carbynoid Structures (eds Heimann, R. B. et al.) (Kluwer Academic Publishers, 1999).

[12]. Horný, L., Petraco, N. D. K. & Schaefer, H. F. III Odd carbon long linear chains HC2n+1H (n=4–11): Properties of the neutrals and radical anions. *J. Am. Chem. Soc. 124, 14716–14720 (2002).*

[13]. Van Zee, R. J., Ferrante, R. F., Zeringue, K. J., Weltner, W. Jr. & Ewing, D. W. Electron spin resonance of the C6, C8, and C10 molecules. *J. Chem. Phys. 88, 3465 (1988).*

[14]. Pan, L., Rao, B. K., Gupta, A. K., Das, G. P. & Ayyub, P. H-substituted anionic carbon clusters CnH− (n≤10): Density functional studies and experimental observations. *J. Chem. Phys. 119, 7705 (2003).*

[15]. Jin, C., Lan, H., Peng, L., Suenaga, K. &Iijima, S. Deriving carbon atomic chains from graphene. *Phys. Rev. Lett. 102, 205501 (2009).*

[16]. Chuvilin, A., Meyer, J. C., Algara-Siller, G. & Kaiser, U. From graphene constrictions to single carbon chains. *New J. Phys. 11, 083019 (2009).*

[17]. Kano, E., Takeguchi, M., Fujita, J.-I. & Hashimoto, A. Direct observation of Pt-terminating carbyne on graphene. *Carbon 80, 382–386 (2014).*

[18]. Banhart, F. Chains of carbon atoms: a vision or a new nanomaterial? Beilstein *J. Nanotechnol. 6, 559–569 (2015).*

[19]. Casari, C. S., Tommasini, M., Tykwinski, R. R. & Milani, A. Carbon-atom wires: 1-D systems with tunable properties. *Nanoscale 8, 4414–4435 (2016).*

[20]. Belau, L. et al. Ionization thresholds of small carbon clusters: tunable VUV experiments and theory. *J. Am. Chem. Soc. 129, 10229–10243 (2007).*

[21]. Lang, N. D. &Avouris, P. Oscillatory conductance of carbon-atom wires. *Phys. Rev. Lett. 81, 3515 (1998).*

[22]. Souza, A. M. C. & Herrmann, H. Theory of local electronic properties and finite-size effects in nanoscale open chains. *Phys. Rev. B 77, 085416 (2008).*

[23]. Li, Z. Y. et al. Magnetism and spin-polarized transport in carbon atomic wires. *Phys. Rev. B 80, 115429 (2009).*

[24]. Artyukhov, V. I., Liu, M. &Yakobson, B. I. Mechanically induced metal-insulator transition in carbyne. *Nano Lett. 14, 4224–4229 (2014).*

[25]. Brus, L. Size, dimensionality, and strong electron correlation in nanoscience. *Acc. Chem. Res. 47, 2951–2959 (2014).*

[26]. Kohn, W. & Sham, L. J. Self-consistent equations including exchange and correlation effects. *Phys. Rev. 140, A1133–A1138 (1965).*

[27]. Perdew, J. P., Burke, K. &Ernzerhof, M. Generalized gradient approximation made simple. *Phys. Rev. Lett. 77, 3865–3868 (1996).*

[28]. Becke, A. D. Density-functional thermochemistry. III. The role of exact exchange. *J. Chem. Phys. 98, 5648–5652 (1993).*

[29]. Wang, C.-W., Hui, K. & Chai, J.-D. Short- and long-range corrected hybrid density functionals with the D3 dispersion corrections. *J. Chem. Phys. 145, 204101 (2016).*

[30]. Grimme, S. Semiempirical hybrid density functional with perturbative second-order correlation. *J. Chem. Phys. 124, 034108 (2006).*

[31]. Chai, J.-D. & Mao, S.-P. Seeking for reliable double-hybrid density functionals without fitting parameters: the PBE0-2 functional. *Chem. Phys. Lett. 538, 121–125 (2012).*

[32]. Cohen, A. J., Mori-Sánchez, P. & Yang, W. Challenges for density functional theory. *Chem. Rev. 112, 289–320 (2012).*

[33]. Gryn'ova, G., Coote, M. L. &Corminboeuf, C. Theory and practice of uncommon molecular electronic configurations. WIREs Comput. *Mol. Sci. 5, 440–459 (2015).*

[34]. Chai, J.-D. Density functional theory with fractional orbital occupations. J. Chem. Phys. 136, 154104 (2012). www.nature.com/scientificreports/ Scientific Reports | 7: 4966 | DOI:10.1038/s41598-017-05202-6 1 0

[35]. Chai, J.-D. Thermally-assisted-occupation density functional theory with generalized-gradient approximations. *J. Chem. Phys. 140, 18A521 (2014).*

[36]. Chai, J.-D. Role of exact exchange in thermally-assisted-occupation density functional theory: a proposal of new hybrid schemes. *J. Chem. Phys. 146, 044102 (2017).*

[37] Wu, C.-S. & Chai, J.-D. Electronic properties of zigzag graphene nanoribbons studied by TAO-DFT. *J.Chem.Theory Comput.11,2003–2011 (2015)*

[37]. Tsivion, E., Long, J. R. & Head-Gordon, M. Hydrogen physisorption on metal-organic framework linkers and metalated linkers: a computational study of the factors that control binding strength. *J. Am. Chem. Soc. 136, 17827–17835 (2014)*.

[38]. Grimme, S. Semiempirical GGA-type density functional constructed with a long-range dispersion correction. *J. Comput. Chem. 27, 1787–1799 (2006)*.

[39]. Boys, S. F. & Bernardi, F. The calculation of small molecular interactions by the differences of separate total energies. Some procedures with reduced errors. *Mol. Phys. 19, 553–566 (1970)*.

[40] Hui, K. & Chai, J.-D. SCAN-based hybrid and double-hybrid density functionals from models without fitted parameters. *J. Chem.Phys. 144, 044114 (2016).*

[41] Rivero, P., Jiménez-Hoyos, C. A. & Scuseria, G. E. Entanglement and polyradical character of polycyclic aromatic hydrocarbonspredicted by projected Hartree-Fock theory. *J. Phys. Chem. B 117, 12750–12758 (2013)*

[42] Löwdin P.-O., Shull H. (1956). Natural orbitals in the quantum theory of two-electron systems. *Phys. Rev. 101, 1730–1739. 10.1103/PhysRev.101.1730* [CrossRef] [Google Scholar]

[43] Chai J.-D. (2012). Density functional theory with fractional orbital occupations. *J. Chem. Phys. 136:154104. 10.1063/1.3703894* [PubMed] [CrossRef] [Google Scholar]

[44] Chai J.-D. (2014). Thermally-assisted-occupation density functional theory with generalized-gradient approximations. *J. Chem. Phys. 140:18A521. 10.1063/1.4867532* [PubMed] [CrossRef] [Google Scholar]

[45] Chai J.-D. (2017). Role of exact exchange in thermally-assisted-occupation density functional theory: a proposal of new hybrid schemes. *J. Chem. Phys. 146:044102. 10.1063/1.4974163* [PubMed] [CrossRef] [Google Scholar]

[46] Rivero P., Jiménez-Hoyos C. A., Scuseria G. E. (2013). Entanglement and polyradical character of polycyclic aromatic hydrocarbons predicted by projected Hartree-Fock theory. *J. Phys. Chem. B 117, 12750–12758. 10.1021/jp401478v* [PubMed] [CrossRef] [Google Scholar]

[47] Wu C.-S., Chai J.-D. (2015). Electronic properties of zigzag graphene nanoribbons studied by TAO-DFT. *J. Chem. Theory Comput. 11, 2003–2011. 10.1021/ct500999m* [PubMed] [CrossRef] [Google Scholar]

[48] Seenithurai S., Chai J.-D. (2016). Effect of Li adsorption on the electronic and hydrogen storage properties of acenes: a dispersion-corrected TAO-DFT study. Sci. Rep. 6:33081. 10.1038/srep33081 [PMC free article] [PubMed] [CrossRef] [Google Scholar]

[49] Seenithurai S., Chai J.-D. (2017). Effect of Li termination on the electronic and hydrogen storage properties of linear carbon chains: a TAO-DFT study. Sci. Rep. 7:4966. 10.1038/s41598-017-05202-6 [PMC free article] [PubMed] [CrossRef] [Google Scholar]

[50] Seenithurai S., Chai J.-D. (2018). Electronic and hydrogen storage properties of Li-terminated linear boron chains studied by TAO-DFT. Sci. Rep. 8:13538. 10.1038/s41598-018-31947-9 [PMC free article] [PubMed] [CrossRef] [Google Scholar]

[51] Seenithurai S., Chai J.-D. (2019). Electronic properties of linear and cyclic boron nanoribbons from thermally-assisted-occupation density functional theory. Sci. Rep. 9:12139. 10.1038/s41598-019-48560-z [PMC free article] [PubMed] [CrossRef] [Google Scholar]

[52] Niu, J., Rao, B. K. & Jena, P. Binding of hydrogen molecules by a transition-metal ion. Phys. Rev. Lett. 68, 2277–2280 (1992).

[53] Niu, J., Rao, B. K., Jena, P. & Manninen, M. Interaction of H 2 and He with metal atoms, clusters, and ions. Phys. Rev. B 51, 4475–4484(1995).

[54] Froudakis, G. E. Why alkali-metal-doped carbon nanotubes possess high hydrogen uptake. Nano Lett. 1, 531–533 (2001